Dynamical Behavior of High Molecular Weight Polystyrene in the Marginal Solvent 2-Butanone

Wyn Brown* and Johan Fundin

Institute of Physical Chemistry, University of Uppsala, Box 532, 751 21 Uppsala, Sweden

Received January 31, 1991; Revised Manuscript Received April 19, 1991

ABSTRACT: This article reports the dynamic properties of polystyrene in the marginal solvent 2-butanone at both dilute and semidilute concentrations. The first internal mode (τ_1), evaluated by use of dynamic light scattering in the range $0.75 < qR_g < 1.4$, is concentration-independent up to $\approx C^*/2$, with a value agreeing with that predicted by the Zimm nondraining model. Above $\approx C^*/2$, τ_1 decreases monotonically. Semidilute solutions in this system are characterized by the presence of a broad distribution of slow (possibly q-independent) modes in addition to the q^2-dependent gel mode. The concentration dependence of the latter is characterized by $\xi \sim C^{-0.43}$ in agreement with earlier investigations. Renormalization group theory incorporating hydrodynamic screening provides a good description of the dynamic behavior in this marginal solvent system.

Introduction

The static and dynamic properties of polystyrene (PS) in dilute and semidilute solution in thermodynamically good solvents have been explored in some detail by light scattering, neutron scattering, and small-angle X-ray scattering techniques. More recently, light scattering investigations have been extended to solutions in θ solvents.[1-3] Semidilute solutions have been the subject of a recent review article.[4] By comparison, however, solution properties in the important group of solvents referred to as marginal solvents have been neglected.

While the θ state is unambiguously defined in the dilute region with a zero second virial coefficient (A_2), the expression "good" solvent is relative depending on the magnitude of A_2. The term marginal solvent is used for solvents characterized by weak excluded-volume interactions and refers to solvents of intermediate quality for a given polymer, in which for example, the scaling exponent in $R_g \sim M^\nu$ lies between 0.5 (θ) and 0.6 (good). Both ethyl acetate and 2-butanone are usually regarded as marginal solvents for polystyrene in the weakness of their binary interactions resulting in radii of gyration and A_2 values substantially lower than found in typical good solvents such as benzene or tetrahydrofuran. When discussing semidilute solutions in marginal solvents, some authors have used two length scales in endeavors to describe the thermodynamic interactions between polymer chains.[5-7] One is the usual screening length (ξ), (which may be either the static length (ξ_s) or the dynamic length (ξ_h)) and the other is the length scale (ξ_τ) over which excluded-volume effects are not significant; i.e., swelling is only found for distances greater than ξ_τ. ξ depends only on concentration, while ξ_τ changes with solvent quality, which may be altered by, for example, changing the temperature. The temperature–concentration (T–C) diagram introduced by Daoud and Jannink[5] provides a convenient means of representation. In thermodynamically good solvents where excluded-volume effects dominate, $\xi \gg \xi_\tau$. Marginal solvents may be considered to correspond to the situation where these length scales have become comparable, when the concentration is increased $\xi < \xi_\tau$. This means that the chains become nearly ideal on all length scales and such systems may then be treated by mean field theory, as was done in the classical work of Edwards.[8,9] It should be noted that, although the excluded-volume effects are weak, they are not absent and binary interactions between chains still dominate in marginal solvents. This situation contrasts with poor (θ) solvents in which ternary interactions dominate over the binary interactions. The two regimes are sometimes distinguished as subdivisions of the mean field region and are characterized by $\xi \sim C^{-1/2}$ (marginal) and $\xi \sim C^{-1}$ (θ).

Schaefer et al.[6,7] have also discussed the possibility of transitions between regimes varying in solvent quality. These workers, ignoring possible influences of entanglements, supposed on the basis of the T–C diagrams that even PS in its classically good solvents (e.g., benzene or THF) will exhibit transitions to marginal characteristics and eventually show θ-like behavior at sufficiently high concentrations. However, comparison of a large body of experimental data does not provide any convincing support for this contention since a common power law is found for concentrations up to $\approx$30% in a variety of good solvents.[4] We consider that the presumed crossover to various regimes of solvent quality when the concentration is changed is an artifact caused by examination of a too-limited range of concentration. Although the scaling exponent of −0.5 is not observed in marginal solvents (the value is closer to −0.4[6]), there is clear evidence that flexible polymers in marginal solvents differ substantially in characteristics compared to both good solvents and the limiting behavior of chains observed in θ solvents. Such systems thus require more thorough examination.

The present article is directed to an examination of the system PS in 2-butanone. Other recent papers on PS in marginal solvents are those reporting dynamic light scattering (DLS) experiments on PS in ethyl acetate.[10-14] As was pointed out in ref 4, it is imperative to recognize the complexity of the relaxation time distribution in marginal solvents. Not only is there a fast mode characterizing the transient gel (or "blob") dynamics, but there is also a broad decay of a slowly relaxing q-independent component(s) which, by analogy to the θ systems, one may assume is related to viscoelastic relaxation processes. For the characterization of such a system it is important to make DLS experiments over a wide range of sampling times and treat with circumspect previous analyses using either the cumulants method or a forced fit to a single exponential. The presence of slow, q-independent, mode(s) suggests that the influence of entanglements cannot be neglected in marginal solvents. Recent studies on PS in cyclohexane at temperatures up to 65 °C[3] (at which temperatures this solvent is of marginal quality for PS) revealed the significant role played by entanglements.

The present paper is divided into two parts: In the first, various methods are used to isolate the internal

0024-9297/91/2224-5171$02.50/0

mode(s) of the single PS coil over a range of concentration in the dilute regime since it is relevant to examine how current methods of data analysis compare with those employed earlier. It is of interest to do this to remove some ambiguities resulting from conflicting reports in earlier works (e.g., refs 15–17), to examine at what point τ_1 becomes dependent on polymer concentration, and to examine the nature of this dependence. In the second part, the properties of the marginal system are examined in semidilute solution and the results from both dynamic light scattering and sedimentation are analyzed in terms of renormalization group theory.[18]

Experimental Section

The polystyrene sample ($M = 3.17 \times 10^6$) was synthesized at Risø National Laboratory, Roskilde, Denmark, and characterized by gel permeation chromatography and static light scattering. Values of molecular weight, radius of gyration, and intrinsic viscosity are given below.

Static Light Scattering. Intensity light scattering measurements were made using a photon-counting apparatus supplied by Hamamatsu to register the scattered signal. The light source was a 3-mW He–Ne laser. The optical constant for vertically polarized light is $K = 4\pi^2 n_o^2 (dn/dc)^2/(N_A\lambda^4)$, where n_o is the solvent refractive index, dn/dc is the measured refractive index increment (0.208 mL g^{-1} at 25 °C and 633 nm), and λ is the wavelength in vacuo (633 nm). The reduced scattered intensity, KC/R_θ, was derived, where C is the concentration and R_θ is the Rayleigh ratio obtained through calibration using benzene; $R_{90} = 8.51 \times 10^{-6}$.[19] Measurement of the angular dependence of KC/R_θ at $C \to 0$ gave the radius of gyration, $R_g = 555$ Å. This value is substantially lower than that estimated for polystyrene of the same molecular weight in a good solvent ($R_g = 895$ Å) by using the well-established relationship $R_g = 0.1212 M_w^{0.595}$ [46] and somewhat greater than the θ solvent value 515 Å from the equation $(R_g)_\theta = 0.29 M_w^{0.50}$.[47] The second virial coefficient is 0.7×10^{-4} mL mol g^{-2} compared to the value in a good solvent value of 2.3×10^{-4} mL mol g^{-2} (using the relationship $A_2 = 1.17 \times 10^{-2} M_w^{-0.262}$).[46]

Dynamic light scattering measurements were made using the apparatus and technique described in ref 2. Laplace inversion of the correlation curves was performed by using a constrained regularization program REPES[20] to obtain the distribution of decay times. The algorithm differs in a major respect from CONTIN[21] in that the program directly minimizes the sum of the squared differences between the experimental and calculated $g^2(t)$ functions using nonlinear programming and the a priori chosen parameter "probability to reject" was selected as $P = 0.5$. The decay time distributions were similar to those obtained with CONTIN with a similar degree of smoothing.

Intrinsic viscosity measurements were made at 25 °C using an Ubbelohde capillary viscometer. The value $[\eta]_{25} = 228$ mL g^{-1} was obtained for PS ($M = 3.17 \times 10^6$) in 2-butanone.

Sedimentation velocity measurements were made at 54 000 rpm using an MSE analytical ultracentrifuge (Centriscan 75) equipped with schlieren optics at 25 °C.

The molecular weight was determined by combining sedimentation and diffusion coefficients at infinite dilution and gave the value $M_{s,D} = 3.17 \times 10^6$.

Results and Discussion

Evaluation of Internal Modes. As is well-known, a cumulants evaluation of an effective relaxation rate (Γ_e) leads to a diffusion coefficient that is angle-dependent due to the increasing participation of internal modes at higher angles where $qR_g > 1$. At infinite dilution and $q \to 0$, $D_o = 1.50 \times 10^{-11}$ m^2 s^{-1}.

Figure 1a shows the relationship between the dimensionless decay rate, $\Gamma_e/(q^3kT/\eta_o)$ and qR_g in the PS–2-butanone system. Even at a value of $qR_g \sim 1.5$, a limiting value is approached that agrees approximately with the asymptotic value of 0.053 from the Akcasu–Gurol expression.[22,23] The full and dashed lines in Figure 1a correspond to the expression derived from use of the nonpreaveraged and preaveraged Oseen tensors, respectively. Others have observed that experimental data for PS in good solvents fall close to the above prediction.

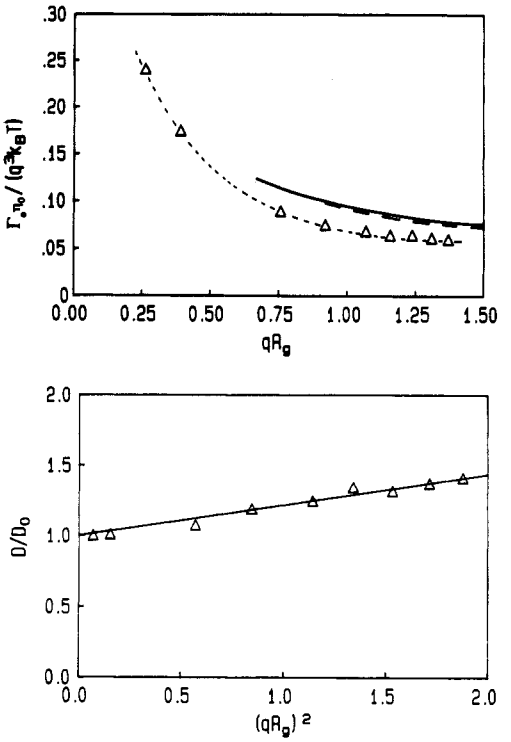

Figure 1. (a, top) The reduced relaxation rate, $\Gamma_e/(q^3kT/\eta_o)$, as a function of qR_g for polystyrene in 2-butanone. The full and dashed lines are, respectively, the Akcasu–Gurol expression[22] with the nonpreaveraged and preaveraged Oseen tensor. (b, bottom) The reduced diffusion coefficient (cumulants) at $C = 4.58 \times 10^{-4}$ g mL^{-1} as a function of $(qR_g)^2$. The slope in eq 1 is given by $C = 0.24$.

We find here that the coefficient C in the equation

$$\Gamma_e(q,0)/q^2D_o = D/D_o = [1 + C(qR_g)^2] \qquad (1)$$

has the value 0.24 (Figure 1b), compared with the predicted value of $C = 0.173$ for PS in good solvents.[24] Since the initial slope will depend on the excluded volume, a decrease in solvent quality should lead to a lower slope in a poorer solvent, however.

Earlier reports[15–17] dealing with the separation of internal modes for large coils in dilute solution have illustrated the difficulties of making such experiments. The amplitudes of the internal mode contributions are small (of the order of a few percent; see Table I) over the q region in which separation from the diffusional component is unambiguous. An earlier investigation[16] had shown that only a very limited range of qR_g with $1 > qR_g < 2$ can be meaningfully employed to extract τ_1. Already for $qR_g \sim 2$ the internal mode peak having the relaxation time $1/(Dq^2 + 2/\tau_1)$ has partially merged with the diffusional peak and cannot then be separated with precision. Moreover, at $qR_g > 2$, the behavior becomes even more complex since groups of internal modes then separate from the main component (containing an admixture of diffusion and the first internal mode) as a distinct peak in the relaxation time distribution. In the following section, experiments used to estimate the relaxation time of the first internal mode are elaborated in some detail to illustrate the utility of various approaches. The data show the exceptional resolution obtainable from DLS data in a demanding situation where a component of low relative amplitude is

Table I
Relaxation Rates, Relative Amplitudes, and Relaxation Times for the Polystyrene ($M_w = 3.17 \times 10^6$)-2-Butanone System from a Bimodal Fit (Equation 2)[a]

Θ, deg	$(qR_g)^2$	$10^{-3}\Gamma_f$, s^{-1}	10^2A_f	$10^{-3}\Gamma_s$, s^{-1}	$10^{-3}(\Gamma_f - \Gamma_s)$, s^{-1}	τ_1, μs
60	0.57	38.3	0.5	2.5	35.9	55.8
75	0.85	32.9	1.7	3.7	29.2	68.5
90	1.14	38.4	3.0	5.0	33.5	59.8
100	1.34	30.9	3.9	5.8	25.0	79.9
110	1.53	42.1	4.9	6.7	35.4	56.5
120	1.71	41.4	5.8	7.5	33.9	59.0
130	1.88	40.5	6.9	8.2	32.3	61.9
						av 63.1

[a] $C = 8 \times 10^{-4}$ g mL^{-1}.

Table II
Relaxation Rates and Relaxation Times for the Polystyrene-2-Butanone System in Table I but with Force Fitting to a Single-Exponential Function (Equation 4)[a]

Θ, deg	$(qR_g)^2$	$10^{-3}\Gamma_f$, s^{-1}	τ, μs
60	0.57	29.7	67.4
75	0.85	28.7	69.8
90	1.14	35.2	56.9
100	1.34	27.0	74.1
110	1.53	37.9	52.9
120	1.71	35.0	57.2
130	1.88	30.3	66.0
			av 63.5

[a] After dividing out the diffusional term in eq 5.

separated from a major component differing little in relaxation time. Three methods are used:

(1) A bimodal fit was used to isolate the fast mode (Γ_f), fixing the slow mode at the experimental relaxation rate (Γ_s) previously determined from measurements of its average value at a series of low angles in the range Θ = 16–22°.

$$g^2(t) - 1 = \beta[A_f \exp(-\Gamma_f t) + A_s \exp(-\Gamma_s t) + B]^2 \quad (2)$$

β is a coefficient accounting for deviations from ideal correlation and B is a base line. The amplitudes of both fast and slow components and the relaxation rate of the fast mode are determined by the fitting program and exemplified in Table I. According to eq 5 below, the relaxation time of the first internal mode is

$$\tau_1 = 2/(\Gamma_f - \Gamma_s) \quad (3)$$

ignoring contributions of higher modes. Table I includes the relaxation rates as a function of angle, the parameter $x = (qR_g)^2$,[25] and the determined relaxation time.

(2) The experimental (normalized) autocorrelation function ($g^2(t)$) was divided by the diffusional term exp($-2q^2Dt$), using the average D value determined at low angles to give a reduced correlation function. Subsequently, the latter was force-fitted to a single-exponential function, including a base line:

$$g^2(t) = \beta[\exp(-\Gamma_f t) + B]^2 \quad (4)$$

τ_1 is then obtained as $\tau_1 = 2/\Gamma_f$, and these values are listed in Table II as a function of angle.

(3) Laplace inversion was performed on the normalized correlation function reduced as under (b), using the program REPES.[20]

Figure 2a shows relaxation time distributions obtained for a concentration of $C = 2.05 \times 10^{-4}$g mL^{-1} at different angles. The small peak on the fast side of the large diffusional peak corresponds to the internal modes. Figure 2b shows the correlation functions before and after division by the diffusional term (where the relaxation rates for this mode, Γ_s, are those given in Table I at each angle), illustrated together with the corresponding Laplace inversion results. Also included in Figure 2b is a simulated autocorrelation function calculated[25] according to

$$g^2(t) = e^{-2Dq^2t}[P_0 + P_{21}e^{-2t/\tau_1} + P_{12}e^{-t/\tau_2} + P_{22}e^{-2t/\tau_2} + ...]^2 \quad (5)$$

where the coefficients P, which depend strongly on the parameter $x = (qR_g)^2$, have been interpolated from the values listed by Perico et al.[26] The values of τ_1 ($2/\Gamma_f$) are listed in Table III at the different angles. The corresponding relaxation time distribution is illustrated. Figure 3 shows the internal mode corresponding to the divided correlation functions at different angles compared to the calculated component obtained by Laplace inversion of the simulated correlation functions. The peak positions on the time axis agree well although the experimental peak is always considerably broader. The latter always contain a small artifactual peak at the extreme short time limit, which appears to derive from the inversion program since it tends to be present in the simulations.

Figure 4a summarizes the τ_1 values as a function of q^2 and Figure 4b τ_1 as a function of concentration in the dilute range, where τ_1 was derived by methods a–c, and compares the values at $q = 0$ with those calculated from the Zimm expression for nondraining random coils:[27]

$$\tau_1 = 0.847M\eta_0[\eta]/RT \quad (6)$$

The various methods used to isolate τ_1 give a high level of agreement. It is necessary, however, to assemble data of exceptionally low noise for any of the methods used in the present case where the purpose is to extract a component of very low intensity having a relaxation time close to that of the major component. Interestingly, with this provision, inversion of the Laplace transform provides equally good solutions, in spite of its so-called ill-conditioned nature and the often-expressed doubt regarding its reliability with an infinite set of possible solutions all of which fit the data within experimental error. There is substantial scatter in the data, which is inevitable considering the very small amplitudes of the internal mode contribution at the low qR_g values employed.

Figure 4a shows that τ_1 is angle-independent, indicating that higher internal modes than the first do not make a significant contribution. Figure 4b shows that τ_1 is approximately concentration-independent over much of the dilute regime up to $\approx C^*/2$ ($C^* \approx 0.45\%$). Agreement with the prediction of the nondraining Zimm model is excellent in this concentration interval, as previously concluded in θ and good solvent polystyrene systems.[16] A similar conclusion was reached by King and Treadway[15] for the same system. The relative amplitude of τ_1 as a function of angle agrees approximately with that evaluated from eq 5.

There are few data in the literature showing the effect of concentration on τ_1. The Muthukumar and Freed theory,[42] taking into account intermolecular interactions, predicts an initial linear concentration dependence for τ_1. Lodge and Schrag[43] concluded from oscillatory flow birefringence data for a low molecular weight polystyrene in Aroclor that τ_1 is essentially concentration-independent in the most dilute range followed by a linear region of higher slope consistent with the conclusion of ref 42.

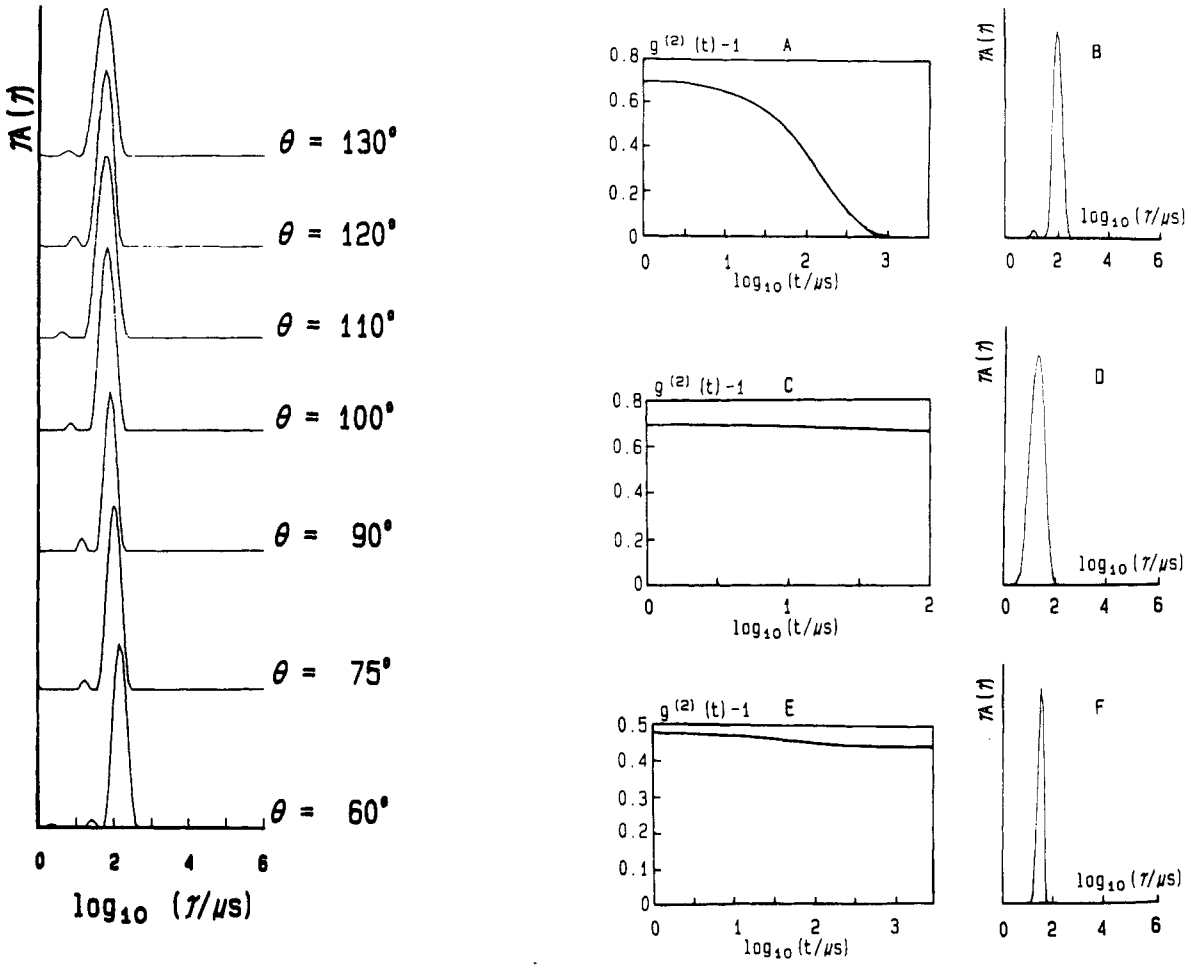

Figure 2. (a, left) Relaxation time distributions for polystyrene in 2-butanone as a function of angle; $C = 2.05 \times 10^{-4}$ g mL^{-1}. The vertical axis is given as $\tau A(\tau)$ to provide an equal area representation of the relative amplitude versus decay time. (b, right) (A) Normalized autocorrelation function ($g^2(t) - 1$); (B) the corresponding decay time distribution ($C = 3.37 \times 10^{-4}$ g mL^{-1}); (C) correlogram in (A) after the main diffusive term is divided out; (D) the corresponding Laplace inversion result from C; (E) simulated correlogram using eq 5 together with coefficients interpolated from Perico et al.;[26] (F) the corresponding inversion of the correlogram in (E).

Table III
Relaxation Rate and Relaxation Times for the Polystyrene–2-Butanone System (as in Tables I and II) but with a Laplace Inversion Routine (See Figure 2)

θ, deg	$(qR_g)^2$	$10^{-3}\Gamma_f$, s^{-1}	τ_1, μs
60	0.57	37.0	54.0
75	0.85	24.3	82.5
90	1.14	41.8	47.9
100	1.34	20.7	96.9
110	1.53	32.8	60.9
120	1.71	30.4	65.7
130	1.88	29.2	68.5
			av 68.0

Another situation is depicted in Figure 4c, which includes data for the concentration dependence of τ_1 over a broader concentration interval, spanning the region above C^*. The hydrodynamically evaluated $C^* = 1/[\eta]$ (see also the slope changes in diffusion and sedimentation plots in Figures 6 and 7a) lies in the vicinity of 0.4%. It is seen that τ_1 decreases significantly above $\simeq C^*/2$, which behavior contrasts with the smooth increase in τ_1 reported by Lodge over a similar concentration range. The origin of this effect is unclear since in the low-qR_g range used here ($qR_g < 1.37$) there should be no interference from modes higher than τ_1 according to the data listed by Perico.[26] SANS measurements of single-coil radii[44] indicate that the radius of gyration decreases strongly with increasing concentration in the dilute regime. However, coil contraction should lead to an increase in the hydrodynamic interactions and thus in τ_1 as has, for example, been demonstrated by Nishio et al.[45] as the θ point is approached. The above data thus provide a strong indication that the relaxation time measured in DLS does not correspond to the viscoelastic relaxation process, which must include a rotational component to the motion of the end-to-end vector under shear flow. There is no such component contributing in the light scattering experiment.

Semidilute Solutions. It has previously been reported[2-4] that, in addition to the expected q^2-dependent mode characterizing the transient gel in semidilute solutions, there exists a broad distribution of slow modes that are q-independent, irrespective of solvent quality. (The results of earlier studies dealing with PS in marginal solvents[10-14] are difficult to reinterpret since the data were fitted with, for example, a bimodal model, which constitutes a gross oversimplification for such complex relaxation time distributions.) It was postulated[28] that these slow modes are related to the viscoelastic properties of the network. A recent article[29] described a comparison of decay time distributions determined from DLS and dynamic mechanical measurements in θ solvents; there are close similarities between them as regards the time range of the slow part of the relaxation spectrum. Typical data for semidilute solutions are shown in Figure 5 giving relaxation time distributions for a solution of PS in 2-butanone of concentration 8.8% ($20C^*$) at a series of q vectors, where the correlation functions have been fitted to the sum of Gaussian and generalized exponential distributions

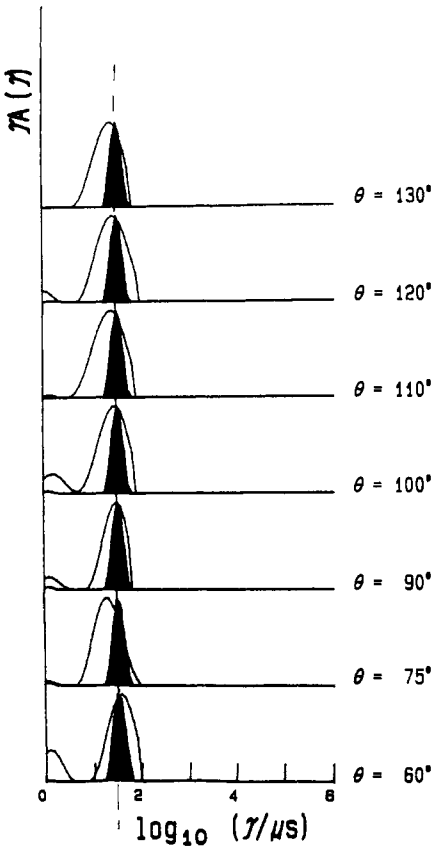

Figure 3. Comparison of the experimental relaxation time distributions with the simulated result (filled peak) for polystyrene in 2-butanone at a concentration of $C = 3.37 \times 10^{-4}$ g mL^{-1}, at different measuring angles.

(GEX) as described in ref 29. The latter distribution has been used to represent the total of the slow modes by a single-peaked function having appropriate skewness, in this case a Pearson distribution.[20] While it is clear that a broad distribution of slower processes is present, the slow peak of low amplitude is very poorly defined and it cannot be established from these data whether or not the slow relaxations in 2-butanone are q-independent. However, evidence has been put forward[4] showing that the corresponding modes in both good[49] and θ solvents[2,3] are q-independent. We would also note that Wang[48] has shown that increasing the polymer concentration beyond the semidilute region results in a gradual decrease in the q^2-dependent diffusion mode, eventually giving rise to a q-independent DLS spectrum characterizing the density fluctuation spectrum of the bulk polymer. There are thus good grounds for anticipating a q-independent part in all semidilute systems.

From viscoelastic theory,[30] one anticipates only a single slow mode related to disentanglement processes, although this is an oversimplification,[31] and a fast mode deriving from internal dynamics of portions of chain between entanglement points. From scattering theory, one expects a single q-independent relaxational mode related to the disentanglement time and a fast diffusive mode (q^2-dependent) due to the osmotic compressibility of the system as well as an elastic contribution from the entanglements, which may be substantial in poor solvents. Wang has recently[48] studied the nature of the dynamic light scattering spectrum of concentrated polymer solutions. He shows that the mutual diffusion involves a coupling of the osmotic pressure fluctuations and the viscoelasticity of the solution. The extent of mixing depends on the frequency and a coupling parameter β, which is related to

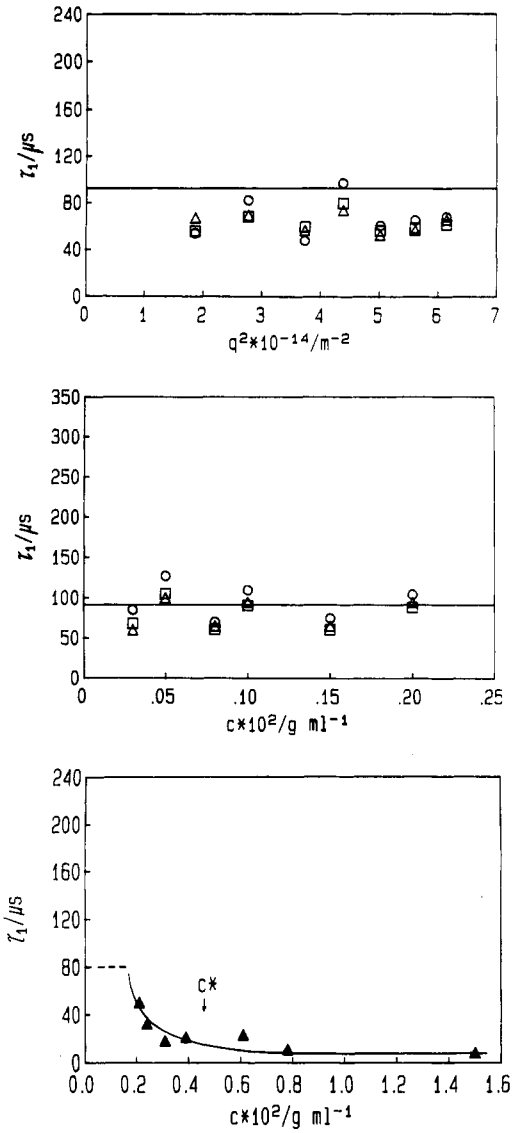

Figure 4. (a, top) Relaxation time of first internal mode (τ_1) as a function of the square of the scattering vector (symbols as in Figure 4b). $C = 8 \times 10^{-4}$ g mL^{-1}. (b, middle) Relaxation time of first internal mode (τ_1) as a function of concentration determined as follows: (1) bimodal fit (Γ_{slow} fixed) (□). (2) forced fit to single exponential after correlation function is divided by diffusional term, $\exp(-2q^2Dt)$ (△). (3) Laplace inversion on divided-out correlation function (○). The values of τ_1 refer to the value at $q = 0$ derived from plots such as that in Figure 4a. (c, bottom) Relaxation time of the first internal mode as a function of concentration spanning the range above and below C^*.

the difference between the partial specific volume of the polymer and that of the solvent. Experiments are currently in progress in this laboratory to explore the dynamical behavior of concentrated solutions and the postulated interrelationship with the viscoelasticity.

Gel Mode. Apart from the uncertainty regarding the slow modes, the relative amplitude and frequency of the fast diffusive mode can be always determined with high precision by using Laplace inversion as described in the Experimental Section. The cooperative diffusion coefficient (D_c) is obtained as

$$D_c = \Gamma/[q^2(1 - \Phi)] \quad (7)$$

Γ is the determined relaxation rate, q is the scattering vector, and $(1 - \Phi)$ corrects for solvent backflow, where Φ is the polymer volume fraction. A logarithmic plot of the

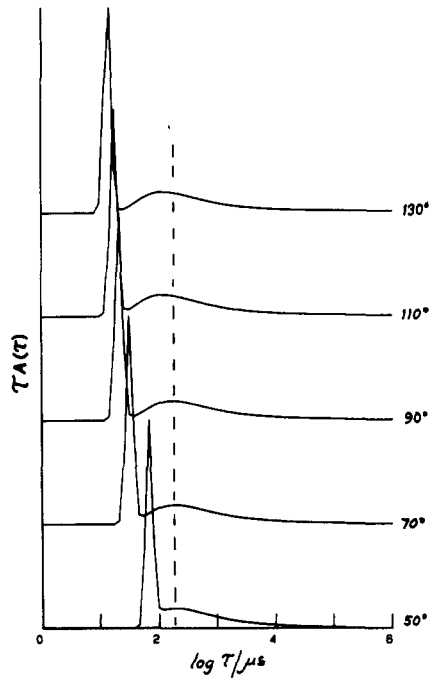

Figure 5. Relaxation time distributions at the measurement angles shown for polystyrene in 2-butanone at $C = 8.8\%$ ($20C^*$). The correlation function has been fitted to the sum of a Gaussian and GEX distribution (see text).

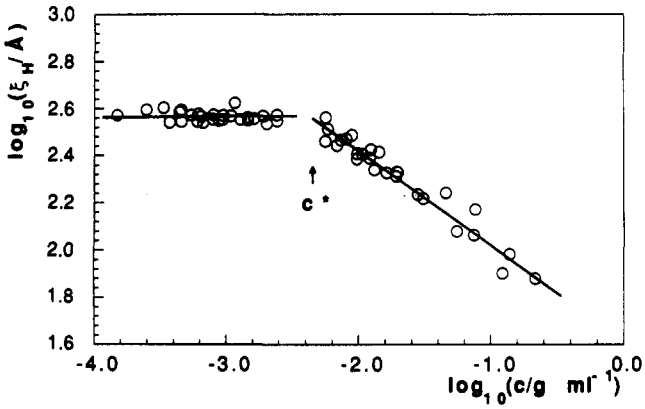

Figure 6. Logarithmic diagram of the concentration dependence of the dynamic correlation length (ξ_H). The data are for a measurement angle of 130°. $C^* = 1/[\eta]$ is indicated.

dynamic correlation length given by

$$\xi_H = kT/6\pi\eta_o D_c \qquad (8)$$

versus concentration spanning the dilute through the semidilute regimes is shown in Figure 6. The demarcation at approximately C^*, when defined as $1/[\eta]$, is of interest, since this is not usually clearly revealed. (The same is true for the sedimentation velocity data (Figure 7).) Above C^* the slope is −0.43. We note that a similar value for the exponent has been given in earlier reports on PS in marginal solvents.[6,7] That an exponent of about −0.4 is observed in marginal solvents has been earlier considered to provide a measure of support for the concept of the blob model involving the two characteristic lengths ξ and ξ_τ thereby justifying the application of mean field theory, which predicts a concentration exponent of −0.5. In this picture the chain is visualized, owing to hydrodynamic screening, as consisting of "blobs" of size ξ_τ within which length the chains are ideal, while at greater length scales full excluded-volume interactions exist. An extensive comparison of experimental data in good solvents, however, casts doubt on this viewpoint. On this model a departure

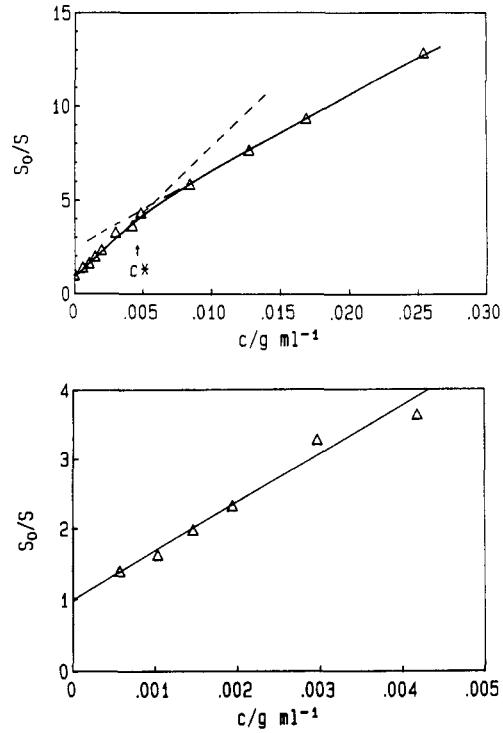

Figure 7. (a, top) Concentration dependence of the reduced sedimentation coefficient (S_o/S) versus concentration. The low concentration portion is shown enlarged in (b) (slope, k_s = 695 mL g^{-1}). $C^* = 1/[\eta]$ is indicated.

from the good solvent power law behavior must occur when ξ falls below the minimum length required for excluded-volume interactions. The latter may be estimated to be in the region of 50 Å for PS in good solvents.[33] However, the experimental value of ξ has decreased to below 10 Å at a concentration of 30%[4] and still the good solvent power law is followed. Similarly, the T–C diagram for PS suggests that above $C \approx 1$–2% in a good solvent such as toluene[7] there should be a transition to marginal solvent behavior and a substantially lower exponent should then be observed—which is clearly not the case. These observations undermine the credibility of the thermal blob model as we have previously pointed out.[4] It may be observed that analysis of static light scattering data[3] gives an ambiguous picture in this situation since it is not possible to distinguish within experimental error between scaling and mean field approximations which require, respectively, exponential and linear fits to the data.

Both the mean field approximation[6-9] and the scaling theory introduced by Daoud and Jannink[5] employing a T–C diagram neglect the effect of entanglements, which may be unjustifiable. Instead we propose that the model proposed by Brochard and de Gennes for θ solvents,[34] which specifically makes provision for the influence of topological interactions, should be generally used for interpretation of dynamic data in poor solvent systems including the so-called marginal solvents and that only in the good solvent limit can one ignore this feature.

Recent contributions have summarized the applicability of the Brochard–de Gennes model to PS in cyclohexane[2-4] and shown that it provides a good description of the data in θ solvents. In this approach, the correlation function is written as the sum of two exponential decays: a fast q^2-dependent mode due to cooperative diffusion in the transient network and a slow q-independent mode related to topological disentanglements. Thus, the cooperative diffusion coefficient determined at high frequencies, where entanglements may be regarded as frozen, should be

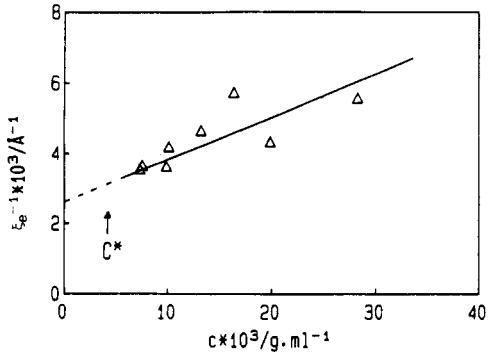

Figure 8. Plot according to eq 9 of the inverse dynamic correlation length versus concentration. The equation of the straight line is given in eq 10.

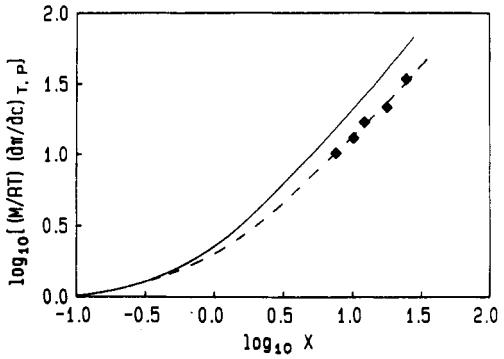

Figure 9. Results for static light scattering for polystyrene in 2-butanone: reduced osmotic compressibility versus the dimensionless parameter X with $X = (16/9)A_2MC$. The continuous line corresponds to the expression of Ohta and Oona.[36]

written as the sum of two terms, one describing the osmotic force in the response to concentration fluctuations and the other giving the effect of the elastic force deriving from the entanglements. In analogy with the reasoning in refs 2 and 3, we write for an effective inverse effective dynamic correlation length (ξ_e)

$$1/\xi_e = 1/\xi_h + f/a \tag{9}$$

where ξ_h is the hydrodynamic correlation length observed when entanglements are absent, f is the number of effective entanglements per binary contact, and a is the size of the monomer. D_c is the cooperative diffusion coefficient measured in the gel regime (i.e., $D_cq_2 \gg T_r^{-1}$, where T_r is the disentanglement time). Figure 8 shows a plot of $1/\xi_e$ versus PS concentration. A linear least-squares fit gives the relationship

$$1/\xi_e = 12.2 \times 10^6 C + 2.6 \times 10^5 \text{ cm}^{-1} \tag{10}$$

This corresponds to $\xi_h = 0.82 \times 10^{-7}$ cm and $a/f = 38$ nm. However, use of a linear expression (eq 10) can be questioned for a marginal solvent since only in the θ state is a finite intercept anticipated according to the reasoning in ref 2. In a marginal solvent both hydrodynamic and gel contributions will be concentration-dependent. A scaling representation (dashed line in Figure 8) with an exponent 0.5 seems more appropriate.

Comparison with Renormalization Group Theory. Results from static light scattering measurements are shown plotted in Figure 9 in the form of the reduced osmotic compressibility as a function of the dimensionless variable X. In this case, we use the close approximation $X = (16/9)A_2MC$, where A_2 is the experimentally determined second virial coefficient and M the weight-average molecular weight. X is close to C/C^* when C^* is defined as $M/N_AR_g^3$. The continuous line represents the behavior

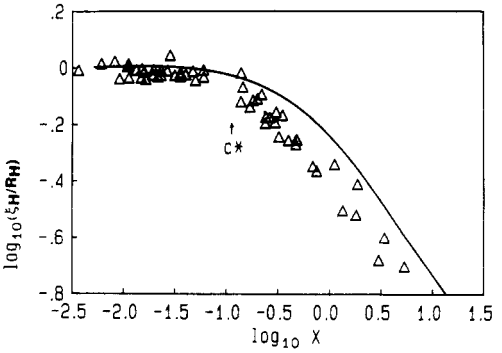

Figure 10. Plot of dynamic light scattering data for polystyrene in 2-butanone according to renormalization group theory with $X = 0.736k_DC$ for a marginal solvent.[38] The continuous line corresponds to the expression of Shiwa[39] including hydrodynamic screening.

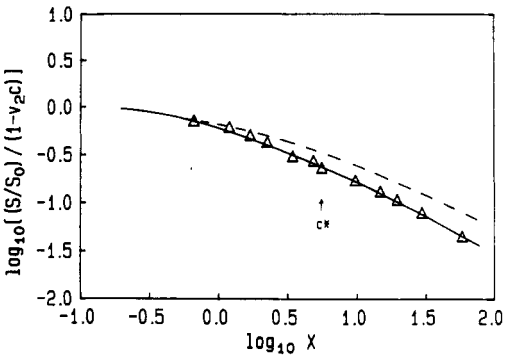

Figure 11. Plot of sedimentation velocity data for polystyrene in 2-butanone according to renormalization group theory with $X = 1.67k_sC$ for a marginal solvent.[41] The broken line is that corresponding to the expression of Shiwa.[39]

predicted by Ohta and Oona.[36] The data support the small systematic deviation observed previously.[37]

The dynamic data have also been treated in the light of renormalization group theory.[18] Here we plot ξ_H/R_H versus the dimensionless overlap parameter X; see Figure 10. The experimental data have been fitted with $X = 0.736k_DC$, where the coefficient is that given for marginal solvents by Nyström and Roots.[38] Here k_D is defined as the coefficient of C in $D_c = D_0(1 + k_DC + ...)$. The value of $k_D = 33.0$ mL g^{-1} found for the present data is used here.[50] The theoretical curve corresponds to the expression of Shiwa with the inclusion of a correction for hydrodynamic screening.[39] A fairly good fit to the experimental data is observed, as has previously been noted for both PS and polyisobutylenes in good solvents.[40]

Figure 11 illustrates a similar comparison with sedimentation velocity data. Here we have used $X = 1.67k_sC$ for the experimental data in accordance with the equations summarized by Nyström and Roots for marginal solvents.[41] Here $S/S_0 = 1/(1 + k_sC)$.

The value of $k_s = 695$ was determined as the initial slope of a plot of S_0/S versus C, as shown in Figure 7b. The broken line is plotted according to a derivation from the expression of Shiwa.[39] These sedimentation data only cover the crossover region between dilute and semidilute regimes and do not allow conclusions to be drawn concerning the semidilute behavior. It would appear to be generally the case that the renormalization group predictions of the dynamic quantities are very satisfactory for describing the crossover to the semidilute regime and also the semidilute concentration dependence of the correlation length, with only small although systematic deviations between theory and experiment.

The ratio ξ_H/R_H may also be obtained by combining sedimentation and osmotic compressibility data by use of the relationship[41]

$$\xi_H/R_H = (S/S_o)^{-1}(RT/M)(\partial\pi/\partial C)^{-1} \quad (11)$$

We observe that, at a given concentration, the ratio (ξ_H/R_H) is systematically smaller by a factor of 2 when eq 11 is used. We have also compared the ξ_H/R_H ratio obtained for a large quantity of data in good solvents[4] with values obtained by combining sedimentation and osmotic compressibility data for polystyrene in good solvents collected by Nyström and Roots. The latter are also systematically smaller by a factor of 2.

Acknowledgment. This work has been supported by the Swedish Natural Science Research Council and the Swedish National Board for Technical Development.

References and Notes

(1) Adam, M.; Delsanti, M. *Macromolecules* **1985**, *18*, 1760.
(2) Nicolai, T.; Brown, W.; Johnsen, R. M.; Stepanek, P. *Macromolecules* **1990**, *23*, 1165.
(3) Nicolai, T.; Brown, W. *Macromolecules* **1990**, *23*, 3150.
(4) Brown, W.; Nicolai, T. *Prog. Colloid Polym. Sci.* **1990**, *268*, 977.
(5) Daoud, M.; Jannink, G. *J. Phys. (Paris)* **1976**, *37*, 937.
(6) Schaefer, D. W.; Joanny, J. F.; Pincus, P. *Macromolecules* **1980**, *13*, 1280.
(7) Schaefer, D. W.; Han, C. C. In *Dynamic Light Scattering*; Pecora, R., Ed.; Plenum: New York, 1985; Chapter 5.
(8) Edwards, S. F. *Proc. Phys. Soc.* **1966**, *88*, 265.
(9) Doi, M.; Edwards, S. F. *The Theory of Polymer Dynamics*; Oxford University Press: Oxford, U.K., 1986.
(10) Munch, J. P.; Candau, S.; Herz, J.; Hild, G. *J. Phys. (Paris)* *38*, 971.
(11) Brown, W. *Macromolecules* **1986**, *19*, 1083.
(12) Brown, W.; Johnsen, R. M. *Macromolecules* **1986**, *19*, 2002.
(13) Brown, W.; Stepanek, P. *Macromolecules* **1988**, *21*, 1791.
(14) Stepanek, P.; Jakes, J.; Brown, W. *Prog. Colloid Polym. Sci.* **1988**, *78*, 1.
(15) King, T. A.; Treadway, M. F. *J. Chem. Soc., Faraday Trans. 2* **1976**, *72*, 1473.
(16) Nicolai, T.; Brown, W.; Johnsen, R. M. *Macromolecules* **1989**, *22*, 2795.
(17) Tsunashima, Y.; Nemoto, N.; Kurata, M. *Macromolecules* **1983**, *16*, 584, 1184.
(18) Freed, K. F. *Renormalization Group Theory of Macromolecules*; Wiley: New York, 1987.
(19) Pike, E. R.; Pomeroy, W. R. M.; Vaughan, A. M. *J. Chem. Phys.* **1975**, *62*, 3188.
(20) Jakes, J.; *Czech. J. Phys. B* **1988**, *38*, 1305.
(21) Provencher, S. W. *Makromol. Chem.* **1979**, *180*, 201.
(22) Akcasu, A. Z.; Gurol, H. J. *J. Polym. Sci., Polym. Phys. Ed.* **1976**, *14*, 1.
(23) Akcasu, A. Z.; Han, C. C.; Benmouna, M. *Polymer* **1980**, *21*, 866.
(24) Burchard, W.; Schmidt, M.; Stockmayer, W. H. *Macromolecules* **1980**, *13*, 580.
(25) Pecora, R. *J. Chem. Phys.* **1965**, *43*, 1562.
(26) Perico, A.; Piaggio, P.; Cumberti, C. *J. Chem. Phys.* **1975**, *62*, 2690, 4911.
(27) Zimm, B. H. *J. Chem. Phys.* **1956**, *24*, 269.
(28) Brown, W.; Nicolai, T.; Hvidt, S.; Stepanek, P. *Macromolecules* **1990**, *23*, 357.
(29) Nicolai, T.; Brown, W.; Hvidt, S.; Heller, K. *Macromolecules* **1990**, *23*, 5088.
(30) Ferry, J. D. *Viscoelastic Properties of Polymers*, 3rd ed. Wiley: New York, 1980.
(31) Raju, V. R.; Menezes, E. V.; Marin, G.; Graessley, W. W.; Fetters, L. J. *Macromolecules* **1981**, *14*, 1668.
(32) Provencher, S. W.; personal communication.
(33) Norisuye, T.; Fujita, H. *Polym. J.* **1982**, *14*, 143.
(34) Brochard, F.; de Gennes, P.-G. *Macromolecules* **1977**, *10*, 1157.
(35) Carlfors, J.; Rymdén, R.; Nyström, B. *Polym. Commun.* **1983**, *24*, 263.
(36) Ohta, T.; Oona, Y. *Phys. Lett.* **1982**, *89A*, 460.
(37) Brown, W.; Zhou, P. *Macromolecules* **1990**, *23*, 1131.
(38) Nyström, B.; Roots, J. *J. Polym. Sci., C: Polym. Lett.* **1990**, *28*, 101.
(39) Shiwa, Y. *Phys. Rev. Lett.* **1987**, *58*, 2102.
(40) Brown, W.; Zhou, P. *Macromolecules* **1991**, *24*, 1820.
(41) Nyström, B.; Roots, J. *J. Polym. Sci., B: Polym. Phys.* **1990**, *28*, 521.
(42) Muthukumar, M.; Freed, K. F. *Macromolecules* **1978**, *11*, 843.
(43) Lodge, T. P.; Schrag, J. L. *Macromolecules* **1982**, *15*, 1376.
(44) Daoud, M.; Cotton, J. P.; Farnoux, B.; Jannink, G.; Sarma, G.; Benoit, H.; Duplessix, R.; Picot, C.; de Gennes, P.-G. *Macromolecules* **1975**, *8*, 804.
(45) Nishio, I.; Swislow, G.; Sun, S.-T.; Tanaka, T. *Nature* **1982**, *300*, 243.
(46) Miyaki, Y.; Einaga, Y.; Fujita, H. *Macromolecules* **1978**, *11*, 1189.
(47) Schmidt, M.; Burchard, W. *Macromolecules* **1981**, *14*, 210.
(48) Wang, C. H. *J. Chem. Phys.*, submitted.
(49) Brown, W.; Stepanek, P. In *Physical Networks*; Burchard, W., Ross-Murphy, S. B., Eds.; Elsevier: New York, 1990; p 111.
(50) The value of k_D obtained by using the equation given by Nyström and Roots[38] is considerably larger (147) for the present molecular weight.

Registry No. PS, 9003-53-6.